FOLIA HISTOCHEMICA ET CYTOBIOLOGICA
Vol. 60, No. 2, 2022
pp. 125–135

ORIGINAL PAPER

VIA MEDICA

Extracts of *Periplaneta americana* alleviate hepatic fibrosis by affecting hepatic TGF-β and NF-κB expression in rats with pig serum-induced liver fibrosis

Dingchun Li[1], Dehong Ma[2], Ye Liu[1], Lihui Liu[1], Yihui Chen[1], Huaie Liu[1], Lu Zhang[1], Jie Lu[1], Kexuan Chen[1], Jing You[1]*, Wu Li[1]*

[1] The First Affiliated Hospital, Kunming Medical University, Yunnan, Kunming 650000, China
[2]Xishuangbanna Dai National Minority Autonomous Prefecture People's Hospital, Xishuangbanna Dai National Minority Autonomous Region, Jinghong 666100, China

Abstract

Introduction. Liver fibrosis is caused by continuous wound healing responses to various harmful stimuli, including viral infection, drugs, alcohol, and autoimmune liver disease. The purpose of this study was to examine the effects of extracts of *Periplaneta americana* (EPA) in rats with pig serum-induced liver fibrosis to preliminarily assess the antifibrotic effect of EPA.

Material and methods. Seventy rats were randomly divided into 7 groups (10 rats in each group): HC, the healthy control group; FC, the fibrotic control group; TL, low-dose EPA treatment group group; TM, medium-dose EPA group; TH, high-dose EPA treatment group; TC1, *Panax notoginseng*/*Salvia mitiorrhiza* treatment control group 1; TC2, colchicine treatment control group 2. TC1 and TC2 were used as the positive control to demonstrate the difference between EPA and the effects of other compounds. The liver fibrosis model was induced by intraperitoneal injection of 0.5 mL pig serum twice a week for 13 weeks in all groups except for the HC group. The hepatic fibrosis model was established at the 7th week, and followingly, the corresponding compounds were administered once a day in all groups for 6 weeks. Alanine aminotransferase (ALT) and aspartate aminotransferase (AST) activity was determined in rat blood serum. We also measured liver fibrosis-related serum markers, including hyaluronic acid (HA), laminin (LN), type III pre-collagen (PC-III) and type IV collagen (IV-C). Hematoxylin and eosin (H&E) and Masson stainings were used to assess liver morphology and determine the stage of fibrosis. Immunohistochemistry was used to detect the protein expression of NF-κB, α-smooth muscle actin (α-SMA), transforming growth factor-β1 (TGF-β1) and tissue inhibitor of metalloproteinase-1 (TIMP-1) in rat liver tissue.

Results. Compared with that of the HC group, the liver tissue of the FC group presented obvious liver damage and collagen deposition. The serum levels of ALT, AST, HA, LN, PC-III and IV-C and the expression of NF-κB, α-SMA, TGF-β1 and TIMP-1 in the FC group were significantly higher than those in the HC group, the EPA treatment groups, the TC1 group and the TC2 group ($P < 0.01$). The levels of serum ALT, AST, HA, LN, PC-III and IV-C and the expression of α-SMA, NF-κB, TGF-β1 and TIMP-1 in the TL, TC1 and TC2 groups were significantly higher than those TM and TH groups ($P < 0.05$). EPA treatment significantly improved liver function, decreased collagen deposition and reversed the pathological changes related to liver fibrosis.

Conclusions. We found that EPA could reduce liver inflammation, suppress liver cell degeneration and necrosis, and reduce the formation of liver fibrous tissue. Its mechanism might be associated with inhibiting the expression of TGF-β1, TIMP-1, NF-κB and α-SMA to block signal transduction pathways in the hepatic fibrosis process. Therefore, EPA, as a traditional Chinese medicine, might be potentially used to prevent and treat hepatic fibrosis in the future. However, further more experiments are necessary to verify its effectiveness and possible signaling pathways.

***Correspondence address:** Jing You and Wu Li
The First Affiliated Hospital, Kunming Medical University,
No. 295 Xichang Road, Kunming 650032, China
Tel/Fax: +86-0871-65324888
e-mail: liwu_893624@163.com

(Folia Histochemica et Cytobiologica 2022, Vol. 60, No. 2, 125–135)

Keywords: Rat; pig-serum hepatic fibrosis; *Periplaneta americana*; NF-κB; α-SMA; TGF-β1; TIMP-1; IHC

Folia Histochem Cytobiol. 2022
10.5603/FHC.a2022.0011
ISSN 0239-8508, e-ISSN 1897-5631

www.journals.viamedica.pl/folia_histochemica_cytobiologica

Introduction

China is the country with the heaviest burden of chronic liver disease in the world, and the incidence of various chronic liver diseases is increasing year by year. Nowadays, about 250 million people live with chronic hepatitis B virus (HBV) infection around the world, of which about 70 million are in China [1]. In addition, there are about 10 million patients with chronic hepatitis C (CHC), about 408 million patients with fatty liver disease, about 330 000 cases with acute liver injury caused by medicine, and about 37 million cases with other liver diseases in China [2–4].

Hepatic fibrosis is caused by wound healing reactions to liver injuries of different etiologies, and it is an important pathological sign in chronic liver disease and a key event in the development of liver cirrhosis [5]. Without timely and effective treatment, hepatic fibrosis easily develops into liver cirrhosis, eventually resulting in liver failure and malignant tumor. Therefore, an in-depth study of the etiology and pathogenesis of liver fibrosis is of great significance for the prevention and treatment of liver fibrosis-related diseases. Although major breakthroughs in the treatment of hepatic fibrosis have been made in experimental research, the potential mechanism of hepatic fibrosis is still being intensively studied. The activation, proliferation, shrinkage, and conversion to fibroblasts of hepatic stellate cells (HSCs) in the progression of liver fibrosis are still primarily studied [6]. With the in-depth study of cell biology and molecular biology research, the traditional view that liver fibrosis in chronic liver disease is irreversible has been gradually changed. Liver fibrosis, even in early liver cirrhosis, was shown to be reversible [7]. Various cytokines and signal pathways are involved in the occurrence and development of liver fibrosis. Transforming growth factor-β (TGF-β) is one of the most important cytokines to promote the development of liver fibrosis [8]. Nuclear factor-κB (NF-κB) plays an important role in the development of liver fibrosis through promoting directly or indirectly the expression of some inflammatory factors (IL-1, TNF-α, IL-6), chemokines, and TGF-β, which could activate HSCs [9].

Our early research showed that extracts from *Periplaneta americana* (EPA, its main components are sugars and amino acids) were beneficial to mice with hepatic fibrosis induced by carbon tetrachloride (CCl4); we also confirmed that *P. notoginseng*/ /*S. miltiorrhiza* tablets and colchicine had an anti-fibrotic effect in rat liver [10–12]. In this study, a hepatic fibrosis model was induced by pig serum and was used to further explore the anti-fibrotic effect of the EPA; we preliminarily clarified the mechanism underlying the anti-liver fibrosis effect of EPA and provided an experimental and theoretical basis for the use of EPA to prevent and treat hepatic fibrosis.

Material and methods

Ethics statement. This study was conducted in accordance with the declaration of Helsinki. This study was conducted with approval from the Ethics Committee of First Affiliated Hospital of Kunming Medical University, Kunming, China.

Animal group and treatment. Five-to-six-week-old male Sprague-Dawley rats weighing 120–150 g were purchased from the Laboratory Animal Care Center of Kunming Medical University. These animals received sufficient food and water and were kept under the same conditions in a temperature-controlled room. They were allowed to acclimate to the environment for one week in the animal cages before the experiments. The seventy rats were randomly divided into 7 groups: HC, the healthy control group; FC, the fibrotic control group; TL, treatment group 1: the low-dose EPA group; TM, treatment group 2: the medium-dose EPA group; TH, treatment group 3: the high-dose EPA group; TC1, treatment control group 1: the *Panax notoginseng*/*Salvia mitiorrhiza* group; and TC2, treatment control group 2: the colchicine group. TC1 and TC2 were used as the positive control to demonstrate the difference between EPA and them. The liver fibrosis model was induced by intraperitoneal injection of 0.5 mL pig serum twice a week for 13 weeks in the animals in all groups except the HC group. The rats in the HC group were injected with an equal amount of normal saline. The hepatic fibrosis model was established in the seventh week, and followingly, the corresponding compounds were administered once a day by intragastric gavage in all groups for 6 weeks. The details of the time course of the experiment were shown in Table 1. During the experiment, the weight, activities, and general condition of all rats were recorded regularly. One day after the final gavage, all rats were sacrificed after anesthesia with ether inhalation. Blood samples were collected from the orbit and were kept at 4°C for further analysis. Then, liver tissue was harvested, fixed with formalin, processed into paraffin blocks, and kept for histopathological examination and immunohistochemical staining.

Experimental materials. Pig serum used in the experiment was purchased from Shanghai Leihao Co., Ltd., preserved in a –20°C refrigerator, and thawed at 4°C before use. The EPA was provided by Kunming SaiNuo Pharmaceutical Co. (Kunming, China) and suspensions were prepared with concentrations of 2.5%, 1.25%, and 0.5% with distilled water, and shaken vigorously before use. *P. notoginseng*/ /*S. miltiorrhiza* tablets were provided by the Preparation Room of the First Affiliated Hospital of Kunming Medical College. An appropriate amount of the tablets was used each

Folia Histochem Cytobiol. 2022
10.5603/FHC.a2022.0011
ISSN 0239-8508, e-ISSN 1897-5631

Table 1. Animal groups and treatment

Groups	Animal treatment	
	The 1st week to the 7th week	The 8th week to the 13th week
HC	Normal saline (0.5 mL, twice a week)	Normal saline (0.2 mL/10 g body weight, once a day)
FC	Pig serum (0.5 mL, twice a week)	Pig serum (0.5 mL, twice a week), and normal saline (0.2 mL/10 g body weight, once a day)
TL	Pig serum (0.5 mL, twice a week)	Pig serum (0.5 mL, twice a week), and the low-dose EPA (0.2 mL/10 g body weight, 0.5% concentration, once a day)
TM	Pig serum (0.5 mL, twice a week)	Pig serum (0.5 mL, twice a week), and the medium-dose EPA (0.2 mL/10 g body weight, 1.25% concentration, once a day)
TH	Pig serum (0.5 mL, twice a week)	Pig serum (0.5 mL, twice a week), and the high-dose EPA (0.2 mL/10 g body weight, 2.5% concentration, once a day)
TC1	Pig serum (0.5 mL, twice a week)	Pig serum (0.5 mL, twice a week), and *P. notoginseng*/*S. mitiorrhiza* (1 g/kg body weight, once a day)
TC2	Pig serum (0.5 mL, twice a week)	Pig serum (0.5 mL, twice a week), and colchicine (0.1 mg/kg body weight, once a day)

time, ground in a mortar and mixed with distilled water to make a suspension of the required concentration, and stored in the refrigerator for later use. Colchicine was provided by Yunnan Botanical Pharmaceutical Co., Ltd., and 1 mg was dissolved in 100 mL distilled water and stored in the refrigerator. Hyaluronic acid (HA), laminin (LN), type III pre-collagen (PC-III), and type IV collagen (IV-C) were assessed with kits for hepatic fibrosis provided by Beijing North Biotechnology Research Institute (Beijing, China).

Serum biochemical analysis. Hepatic fibrosis-related serum markers, including PC-III, IV-C, LN, and HA, were determined by radioimmunoassays with the corresponding reagents provided by Beijing North Biotechnology Research Institute. Liver functional indicators, including alanine aminotransferase (ALT) and aspartate aminotransferase (AST), were detected using blood biochemical test kits according to the manufacturer's instructions for the automatic biochemical analyzer.

Liver histology. After blood was drawn from the rat for later use in biochemical and radioimmunoassay tests, the animal was immediately sacrificed by cervical dislocation and dissected, and the middle of the left lobe, the left lobe, and the front of the right upper lobe of the liver was taken. Liver tissue was fixed in formalin, embedded in paraffin, and routinely cut with microtome into 5 μm-thick slices. The changes in liver pathology, inflammatory activity, collagen fiber proliferation, and liver fibrotic stage were examined and evaluated under a light microscope after hematoxylin and eosin (H&E) staining and Masson staining [2, 13]. The stages of hepatic fibrosis were classified according to the Metavir scoring system [14]. If the stage of liver fibrosis was above the second level, it was assumed that the hepatic fibrosis model was established successfully.

Immunohistochemistry. TGFβ1 antibody (3C11): sc-130348, TIMP-1 antibody (2A5): sc-21734, Smooth Muscle Actin antibody (B4): sc-53142, and NFκB p65 (F-6): sc-8008 were purchased from Santa Cruz Co. (USA), and Masson trichrome staining kit (product ID: MST-8004) was purchased from Fuzhou MXB Biologies Co., Ltd (Fuzhou, China). All the above antibodies were used at 1:100 dilution. According to the operating instructions of the kit, the liver sections were dewaxed, hydrated, treated with hydrogen peroxide, added with primary antibody, secondary antibody, SP solution, developed with DAB stain, counterstained with hematoxylin; dehydrated, mounted, and other steps and observed under a microscope, each field of view contains a portal area plus a hepatic lobule or a fibrous septum. The results were judged by reference to the immunohistochemical color development standard. The positive cells were distributed in brown-yellow cytoplasmic type, and 4 corners and central areas of each section were selected (excluding edge effects) and observed under a 400× field of view; the color rendering index (the percentage of positive cells in the total number of cells) was calculated.

Semiquantitative determination of immunohistochemical staining. The expression of TGF-β1, TIMP, α-SMA, and NF-κB in liver tissue was evaluated under a light microscope after immunohistochemical staining. The deposition of brown granules in the portal region, peripheral central vein, cytoplasm, and interstitial structure indicated positive staining. We observed the color rendering and the range of color development under a high-power microscope until good color rendering for each protein and recorded the degree and range of the color rendering. The mean was the final color rendering index for the expression of each protein [15].

Statistical analysis. Statistical analysis was performed using SPSS 24.0 software. Experimental data were shown as the mean ± SD. Rank data were tested by rank-sum tests, and comparisons between groups were performed by one-way analysis of variance. A = 0.05 and P < 0.05 were considered statistically significant.

Results

General condition of the rats

During the experiment, the hair color, mental state, behavior, water and food intake, other general conditions, and death of the rats were recorded every day, and their weights were recorded weekly. Throughout the whole experiment, the rats in the HC group were lively and responsive, had a good appetite, their body weights increased gradually, and their fur was thick and shiny. In the third week, the rats in the modeling groups showed depressive symptoms, loss of appetite, unkempt hair, reduced activity, reduced water, and food intake, and loss of body weight. In the 6th week, it was found that the rats in the modeling groups were easily irritated and weakened, their nails were prone to bleeding, and some of them had abnormal feces. In the 7th week, the rats in the modeling groups suffered dull and easily shed hair, low activities, loss of appetite, malnutrition, and lethargy, which indicated that the model was established. From the 5th week of treatment on, the general condition of the rats in the TH and TM groups was better than those in the other modeling groups. After the 6-week treatment of the corresponding compounds in all modeling groups, the symptoms mentioned above were alleviated to varying degrees except for the FC group. Among the modeling groups with alleviated symptoms, the TH group performed best, and the TC2 group performed worst. In addition, two rats died in the FC group, one rat died in the TC1 group, one rat died in the TC2 group, and no rats died in the other groups.

Effects of EPA on serum biochemical parameters affected by chronic pig serum exposure

As shown in Fig. 1, compared with those in the HC group, the serum biochemical indexes (ALT and AST) of rats in the modeling groups significantly increased (P < 0.01), compared to those in the FC group. However, the levels of ALT and AST decreased significantly after treatment with *P. notoginseng*/*S. mitiorrhiza*, colchicine, and different doses of EPA (P < 0.01), and the levels of ALT and AST in the TM and TH groups were significantly lower than those in the TL, TC1, and TC2 groups (P < 0.01). The comparison of the levels of ALT and AST between the TM group and the TH group showed no statistically significant differences, which suggested that liver injury was obviously improved after the treatment with *P. notoginseng*/*S. mitiorrhiza*, colchicine and different doses of EPA, and the anti-fibrotic effects of medium- and high-dose EPA were the best.

Effects of EPA on pig serum-induced hepatic fibrosis in rats

As shown in Fig. 2, compared with those in the HC group, the serum HA, LN, PC-III and IV-C levels (serological indicators of liver fibrosis) in the modeling group significantly increased (P < 0.01), compared with those in the FC group. Of note, the levels of HA, LN, PC-III, and IV-C decreased significantly after treatment with *P. notoginseng*/*S. mitiorrhiza*, colchicine, and different doses of EPA (P < 0.01), and the

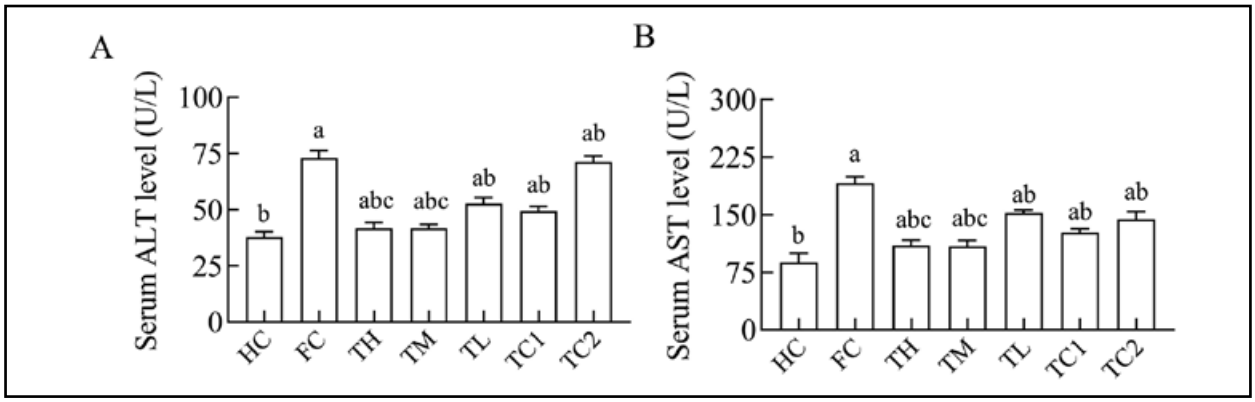

Figure 1. The levels of ALT (A) and AST (B) in the blood serum of the rats in all experimental groups; FC — the fibrotic control group; HC — the healthy control group; TC1 — the *Panax notoginseng*/*Salvia mitiorrhiza* group; TC2 — the colchicine group; TH — the EPA high-dose group; TL — the EPA low-dose group; TM — the EPA medium-dose group Data are presented as the mean ± SD. [a] P < 0.01, compared with the HC group; [b] P < 0.01, compared with the FC; [c] P < 0.01, compared with the TC1, TC2 and TL groups. Abbreviations: ALT — alanine aminotransferase; AST — aspartate transaminase; EPA — extracts from *Periplaneta americana*).

Folia Histochem Cytobiol. 2022
10.5603/FHC.a2022.0011
ISSN 0239-8508, e-ISSN 1897-5631

levels of HA, LN, PC-III, and IV-C in the TM and TH groups were significantly lower than those in the TL, TC1, and TC2 groups ($P < 0.01$). The comparison of the levels of HA, LN, PC-III, and IV-C between the TM group and the TH group showed no statistically significant differences, which suggested that liver fibrosis was obviously improved after the treatment of *P. notoginseng*/*S. mitiorrhiza*, colchicine, and different doses of EPA, and the therapeutic effects of medium- and high-dose EPA were the best.

Macroscopic observations of liver specimens

At the gross dissection, we found that the rats in the HC group had a normal size of the liver, the contour and color of their livers were normal, and their hepatic surface was smooth. Compared with the HC group, the rats in the FC group had a significantly increased liver size, the liver color was pale, the liver textures were harder, and the surface of the liver was bumpy and full of nodules. In addition, the livers of some rats in the FC group were smaller in size. The rats in the TC1, TC2, and TL groups had the above general manifestations of the FC group, but these manifestations of the TC1, TC2, and TL groups were not as clearly pronounced as those of the FC group. Most of the rats in the TM and TH groups had a normal liver size, the texture was soft, the color was slightly gray, and there were no nodular changes on the hepatic surface. The liver samples are shown in Fig. 3.

Effects of EPA on the pathological manifestations of hepatic fibrosis

Under a light microscope, H&E staining and Masson staining of liver sections from the HC group showed the typical structure of the hepatic lobules with hepatocytes arranged in typical plates (Fig. 3). The hepatocytes were uniform in size without signs of degeneration, necrosis, or inflammatory cell infiltration. There were only a few collagen fibers in the vascular wall and portal areas. There was no fibrous tissue hyperplasia between the hepatic lobules, and a false flocculus was not observed.

In the FC group, the liver tissue was seriously damaged, liver cells showed swelling and degeneration,

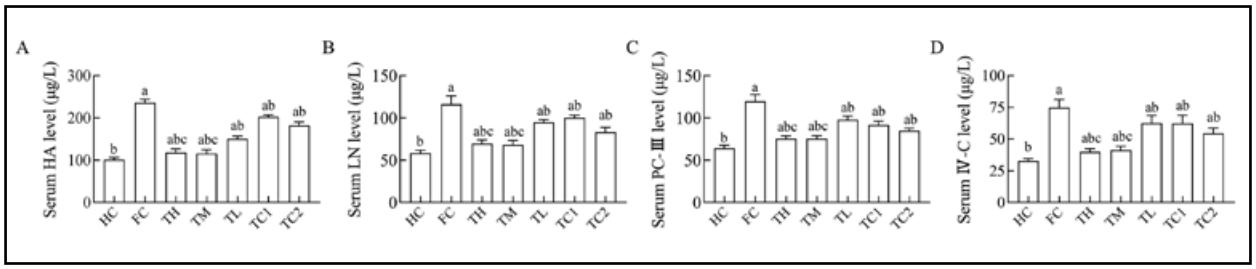

Figure 2. The levels of HA **(A)**, LN **(B)**, PC-III **(C)** and IV-C **(D)** in the blood serum of the rats in all groups. Experimental groups' designation as in the legend to Figure 1. Data are presented as the mean ± SD [a]$P < 0.01$, compared with the HC group; [b]$P < 0.01$, compared with the FC; [c]$P < 0.01$, compared with the TC1, TC2 and TL groups. Abbreviations: HA — hyaluronic acid; IV-C — type IV collagen; LN — laminin; PC-III — type III pro-collagen.

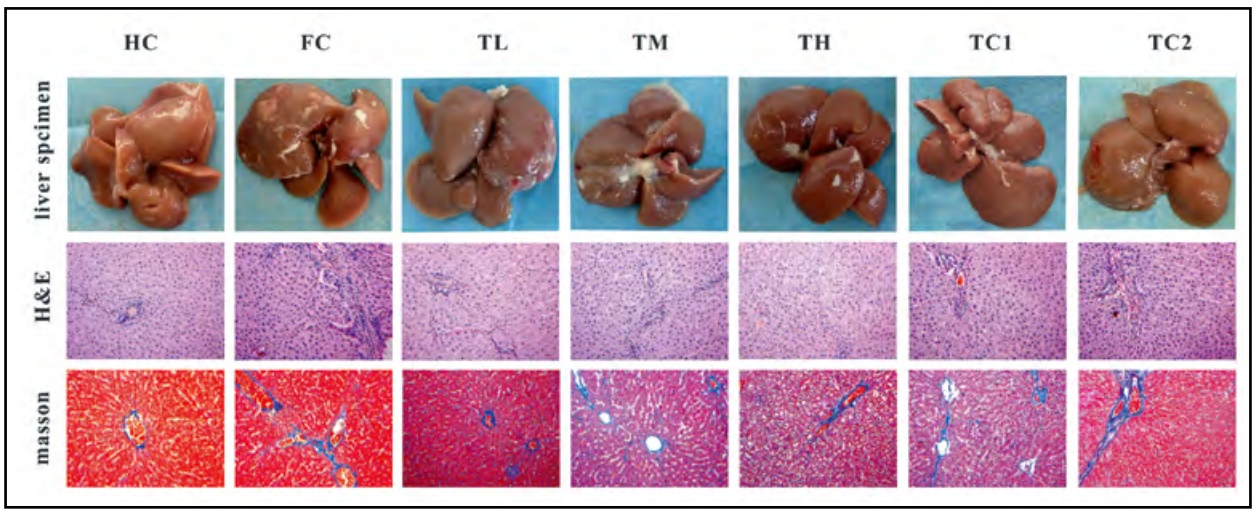

Figure 3. Representative photographs of the liver gross morphology and stained liver sections in all rat experimental groups. Experimental groups' designation as in the legend to Figure 1. Magnifications: H&E and Masson staining — 200×.

Folia Histochem Cytobiol. 2022
10.5603/FHC.a2022.0011
ISSN 0239-8508, e-ISSN 1897-5631

Table 2. The liver inflammation activity grades (G) and fibrosis stages (S) of the rats in all groups

Groups	N	G						S				
		G0	G1	G2	G3	G4		S0	S1	S2	S3	S4
HC	10	10	0	0	0	0^{b}		10	0	0	0	0^{b}
FC	8	0	2	3	3	0^{a}		0	0	1	3	4^{a}
TH	10	2	5	3	0	0^{abc}		0	3	5	2	0^{abc}
TM	10	2	6	2	0	0^{abc}		0	3	6	1	0^{abc}
TL	9	1	3	3	2	0^{ab}		0	1	4	3	1^{ab}
TC1	9	1	3	4	1	0^{ab}		0	1	4	4	0^{ab}
TC2	10	0	3	5	2	0^{ab}		0	2	4	4	0^{ab}

FC — the Fibrotic Control group; HC — the Healthy Control group; TL — the low-dose EPA group; TC1 — the Panax notoginseng/Salvia mitiorrhiza group; TC2 — the colchicine group. (TC2); TH — the high-dose EPA group; TM — the medium-dose EPA group. G — Histological activity, G0–G4; S — fibrosis stage, S0–S4; $^{a}P < 0.01$, compared with the healthy control group (HC); $^{b}P < 0.01$, compared with the fibrotic control group (FC); $^{c}P < 0.01$, compared with the TC1, TC2 and TL groups.

the liver lobules were necrotic, and the majority of the portal tracts were expanded and full of collagen fibers and fibrous septa encircled the hepatic lobule. Moreover, the fibrous septa destroyed the structure of the hepatic lobules, and some of them formed pseudolobules (Fig. 3). Compared with that in the FC group, the liver tissue in the TC1, TC2, and TL groups showed less inflammatory cell infiltration, degeneration, and necrosis of hepatocytes and reduced fibrous hyperplasia. The lobular structure was approximately normal, and the liver tissue in the TM and TH groups showed few inflammatory cells and mild fibrous hyperplasia limited to the portal areas. The pathological features of the liver tissues in the TM and TH groups were less expressed than those in the TL, TC1, and TC2 groups (Fig. 3).

Effects of EPA on liver inflammation and the stage of fibrosis

We performed pathological staging of liver tissue based on the Scheuer score [16]. The results are shown in Table 2. We performed the comparison of inflammatory activity grade (G) and liver fibrosis stage (S) between the HC group and the modeling groups, and the rank-sum test showed that there were significant differences ($P < 0.01$). Compared with that of the FC group, the degree of histological activity and fibrosis stages were reduced significantly after the treatment of rats with EPA, *P. notoginseng*/*S. mitiorrhiza* and colchicine ($P < 0.01$). Compared with those in the TC1, TC2, and TL groups, the signs of liver inflammation and fibrosis in the TM and TH groups were improved, while the comparison of the liver inflammation and fibrosis between the TM group and the TH group showed no statistically significant differences.

Effects of EPA on the expression of TGF-β1, TIMP-1, NF-κB, and a-SMA in liver tissue

As shown in Fig. 4, the expression of α-SMA, NF-κB, TGF-β1, and TIMP-1 was the weakest in the HC group. A small amount of α-SMA was expressed in the arterial and venous walls of the portal areas. There was a low level of NF-κB expression around the hepatocyte circumference, wall of interlobular blood vessels, and stromal cells around the wall of the bile duct. Only a few TGF-β1-immunoreactive sites were found in the intercellular spaces between hepatocytes, and the expression of TIMP-1 was only occasional in the HC group. As shown in Table 3, the proportion of α-SMA, NF-κB, TGF-β1, and TIMP-1 positive cells in the rat liver tissues of the FC group was significantly higher than that of the HC group ($P < 0.01$).

In the FC group, α-SMA was highly expressed in the portal areas, inflammatory cells' infiltration areas, and hepatocytes near the fibrous septum (Fig. 4), which strongly suggested the activation of HSCs. NF-κB was also strongly expressed, and deposited in these areas, including the hepatic lobule, around the hepatic sinusoids and hepatocytes, the confluence area, and the fibrous septum area. The intensely stained areas were observed in the hepatic lobules around the hepatic sinusoids, and hepatocytes. There were also sheet-like fusion areas in the portal area and fibrous septum area. The blood vessel walls were strongly stained. The expression of NF-κB in the TH and TM groups decreased. Only moderately stained cells were observed around the hepatic sinuses, some of which were in small flakes. A small number of lightly and yellow-stained cells were observed in the liver cells and the portal area. TGF-β1 was highly expressed in hepatocytes and mainly distributed around the portal vein, portal area, fibrous septa, and other fibrotic

Folia Histochem Cytobiol. 2022
10.5603/FHC.a2022.0011
ISSN 0239-8508, e-ISSN 1897-5631

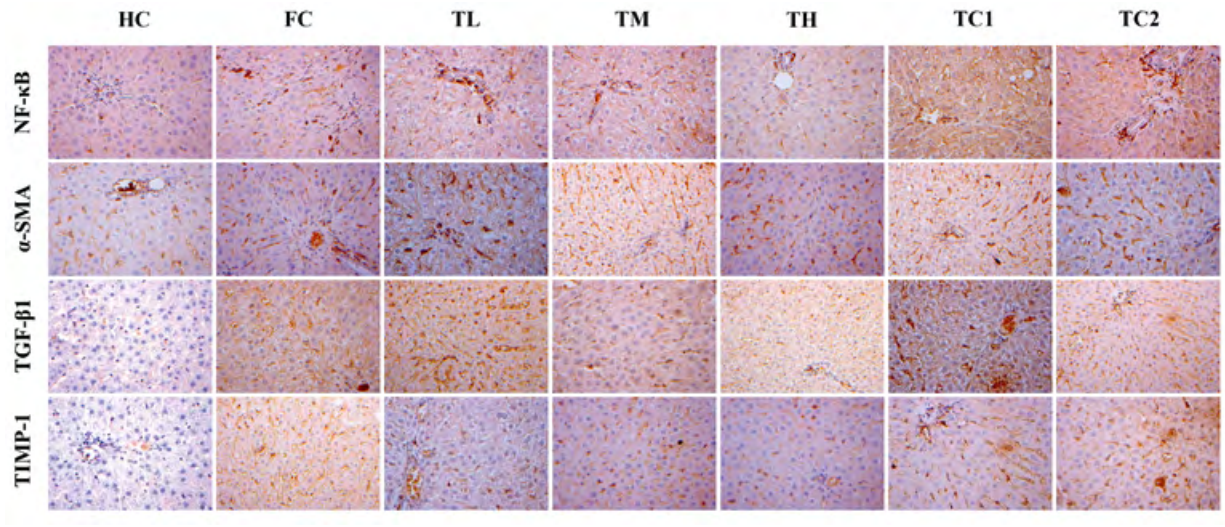

Figure 4. The expression of NF-κB, α-SMA, TGF-β1 and TIMP-1 in the liver sections in all rat experimental groups was determined by immunohistochemistry. Experimental groups' designation as in the legend to Figure 1. Magnification: 400×.

Table 3. The expression levels of TGF-β1, TIMP-1, α-SMA and NF-κB in the liver tissue of rats in all groups

Groups	N	The color rendering index			
		TGF-β1	TIMP-1	NF-κB	α-SMA
HC	10	0.69 ± 0.07^{b}	0.36 ± 0.04^{b}	1.38 ± 0.90^{b}	2.06 ± 0.20^{b}
FC	8	6.53 ± 0.57^{a}	8.19 ± 0.33^{a}	9.04 ± 1.30^{a}	8.69 ± 1.69^{a}
TH	10	2.04 ± 0.23^{abc}	1.77 ± 0.18^{abc}	3.24 ± 0.80^{abc}	4.04 ± 0.66^{abc}
TM	10	2.02 ± 0.30^{abc}	2.09 ± 0.22^{abc}	3.29 ± 0.76^{abc}	4.16 ± 0.76^{abc}
TL	9	4.82 ± 0.60^{ab}	5.49 ± 0.34^{ab}	6.53 ± 0.85^{ab}	6.81 ± 0.82^{ab}
TC1	9	3.76 ± 0.30^{ab}	3.58 ± 0.32^{ab}	5.87 ± 0.82^{ab}	5.81 ± 0.77^{ab}
TC2	10	3.14 ± 0.25^{ab}	2.93 ± 0.27^{ab}	5.34 ± 0.87^{ab}	5.33 ± 0.80^{ab}

FC — the Fibrotic Control group; HC — the Healthy Control group; TC1 — the Panax notoginseng/Salvia mitiorrhiza group; TC2 — the colchicine group (TC2); TH — the EPA high-dose group; TL — the EPA low-dose group; TM — the EPA medium-dose group. $^{a}P < 0.01$, compared with the healthy control group (HC); $^{b}P < 0.01$, compared with the fibrotic control group (FC); $^{c}P < 0.01$, compared with the TC1, TC2 and TL groups.

areas, as well as in periportal parts of hepatic lobules (Fig. 4). The proportion of TIMP-1-positive cells (Fig. 4) in the rat liver tissues was high as compared to normal liver tissue and was mainly concentrated in the epithelial cells of the vascular wall and bile ducts, the surrounding stromal cells, and the cytoplasm of some hepatocytes.

Compared with those in the FC group, the expression of α-SMA, NF-κB, TGF-β1, and TIMP-1 in liver tissue significantly decreased after treatment of rats with EPA, *P. notoginseng*/*S. mitiorrhiza* and colchicine ($P < 0.01$) (Table 3). Compared with those in the TL, TC1, and TC2 groups, the expression of α-SMA, NF-κB, TGF-β1, and TIMP-1 in the TM and TH groups showed a significant decrease ($P < 0.05$) (Table 3), while there was no significant statistical difference in the expressions of α-SMA, NF-κB, TGF-β1 and TIMP-1 between the TM group and the TH group ($P > 0.05$).

Discussion

Liver fibrosis is a serious health problem worldwide, resulting from a sustained wound healing response to various chronic liver injuries caused by different stimuli, including viral infections, drugs, alcohol consumption, cholestasis, autoimmune hepatopathy, and genetic metabolic diseases [17]. Liver fibrosis leads to the destruction of the normal liver structure and impaired organ function, causes liver failure, and subse-

quently results in cirrhosis [18], and its persistence can result in the progression of hepatocellular carcinoma [19]. This condition is characterized by the excessive accumulation of the extracellular matrix (ECM) [20, 21]. HSCs have important roles in the regulation of liver function and hepatic fibrosis [22–24].

Traditional Chinese medicine is effective in the treatment of some chronic diseases, and some Chinese herbs have been proven to prevent fibrogenesis [25]. EPA is a traditional Chinese medicine component extracted from *P. americana* using modern technologies. The preliminary results in our previous studies [11, 12] showed that EPA could significantly reduce the serum levels of ALT and AST and decrease the levels of serum HA, LN, PC-III, and IV-C in a CCl4-induced hepatic fibrosis model. Moreover, EPA could reduce the degeneration and necrosis of liver cells, reduce the deposition of collagen fibers in liver tissue, and reshape the ultrastructure of the liver tissue [10–12, 26–28]. These results showed that this therapy could improve the degree of liver fibrosis in rats and might promote the prevention and treatment of liver fibrosis [11]. However, whether these effects can be repeated in other models and the underlying mechanism are necessary to do further study in the future.

In our present study, the immune hepatic fibrosis model was induced by pig serum administration to explore the antifibrotic effect of EPA and perform further research on its mechanism by detecting liver fibrosis-related factors. Our results showed that the general condition and macroscopic characteristics of the liver specimens of the rats in the EPA treatment groups were significantly better than those in the FC group, and the TM and TH groups had improved parameters compared with the TL, TC1 and TC2 groups. The levels of ALT and AST in the TH and TM groups were significantly lower than those in the TL, TC1, and TC2 groups. The levels of HA, LN, PC-III, and IV-C in serum of the EPA treatment groups, the TC1 group, and the TC2 group were significantly lower than those of the FC group. The levels of HA, LN, PC-III, and IV-C in the TH and TM groups were lower than those in the TL, TC1, and TC2 groups. These results suggested medium- and high-dose EPA might significantly improve liver functions and reduce live fibrosis. HE staining and Masson staining results showed that the damage to liver tissues was more serious in the FC group. Compared with the other modeling groups, there were fewer inflammatory cells and fibrous hyperplasia in hepatocytes in the TH and TM groups, in which hepatic fibrosis was confined to the portal area.

These parameters in the TH and TM groups were significantly better than those in the FC, TL, TC1, and TC2 groups. There were significant differences in G and S compared between the treatment (EPA, *P. notoginseng*/*S. mitiorrhiza*, and colchicine) groups and the FC group. The degree of G and S in the TH and TM groups was less severe than that in the TL, TC1, and TC2 groups.

Our results demonstrated that EPA also reduced serum levels of ALT and AST and decreased hepatic fibrosis-related indexes in rats with immune fibrosis of the liver. Histopathological HE and Masson staining showed that EPA could significantly improve liver injury and decrease the grade of hepatic fibrosis. The therapeutic effects in rats in the TH and TM groups were better than those in the TL group. This finding is consistent with our previous research results in a CCl4-induced liver fibrosis model in rats, confirming that EPA has a therapeutic effect on hepatic fibrosis in rats [10–12]. However, the difference between the previous and current experimental model was that previously rats were given EPA or other control drugs during establishing the CCl4-induced liver fibrosis model, which was a preventive intervention, while currently rats were given EPA or other control drugs after the successful establishment of pig serum-induced immune liver fibrosis model, which was a therapeutic intervention. The successful treatment by EPA in the pig serum-induced hepatic fibrosis model demonstrated that EPA could help reverse experimental liver fibrosis. Thus, EPA is effective in the prevention and treatment of hepatic fibrosis.

Many studies have shown that activated HSCs are the main cells that promote the synthesis of ECM and play an important role in the development of liver fibrosis in the advanced stages. The activation of HSCs, the production and activation of matrix metalloproteinases (MMPs), and the expression of TIMPs are the key factors in determining the progression and reversion of liver fibrosis [29, 30].

TGF-β1 is one of the strongest liver fibrosis--promoting factors [31, 32]. During the development of fibrosis, TGF-β1 stimulates the positive feedback mechanism of TGF-β1 secreted by HSCs through an autocrine mechanism [33]. Collagen synthesis of HSCs is strongly stimulated by TGF-β1 and leads to the continuous development of liver fibrosis [34]. TIMPs are the most important family members of enzymes that regulate the activity of extracellular MMPs [35, 36]. During liver fibrosis, TIMP-1 is mainly secreted by the activated HSCs and can be induced by a variety of cytokines [37]. With the development of this condition, TIMP-1 increases progressively, and the specific combination of MMP-1 and TIMP-1 can decrease the activity of TIMP-1 and inhibit the degradation of ECM components, such as collagen I and III, resulting

Folia Histochem Cytobiol. 2022
10.5603/FHC.a2022.0011
ISSN 0239-8508, e-ISSN 1897-5631

in excessive deposition in the liver and acceleration of liver fibrosis [38]. In this present study, the expression of TGF-β1 and TIMP-1 in the liver tissue of the FC group significantly increased, this result is consistent with the positive feedback mechanism between HSC activation and TGF-β1 secretion, this positive feedback promotes the formation and development of immune hepatic fibrosis in rats after pig serum stimulation, and continuously activated HSCs secrete a large amount of TIMP-1, further aggravating liver fibrosis [22, 39]. The color rendering index (CRI) of TGF-β1 and TIMP-1 in the EPA treatment groups was lower than those in the FC group, especially in the TH and TM groups. These results suggested that EPA might inhibit the activation of HSCs and decrease the levels of TIMP-1 through the TGF-β1 signaling pathway.

α-SMA is a marker of the activation of HSCs, and its expression can reflect the degree of activation and proliferation of HSCs [40]. HSC did not express α-SMA under resting conditions. HSCs are activated by inflammatory mediators and cytokines and transformed into fibroblast-like cells (MFB), migrate to the liver injury site, promote the synthesis of ECM, inhibit its degradation, proliferate at a high rate, and synthesize and secrete TIMPs [2, 41–43].

As a nuclear transcription factor, NF-κB is widely present in various cell types and can regulate the gene expression of many cytokines and inflammatory mediators and participate in the immune response, intracellular signal transduction, and other important functions [44, 45]. Under normal conditions, NF-κB combines with an inhibitor of NF-κB (I-κB) to form a trimer complex in the cytoplasm, and it does not affect nuclear transcription. When NF-κB dissociates from I-κB, it can be transferred into the nucleus and regulate gene transcription [46]. The genes encoding inflammatory molecules are NF-κB target genes and regulating the transcription of these inflammatory molecules is the main function of NF-κB [47]. As shown in previous studies, NF-κB can enhance the expression of the pro-inflammatory factors IL-6, TNF-α, CCL-2, and intercellular adhesion molecule 1 (ICAM-1) and participate in liver inflammation through inflammatory cells [48–50]. Activated NF-κB can also enhance the activation of downstream collagen gene expression and play an important role in the pathogenesis and development of liver fibrosis [51].

The results showed that NF-κB was weakly positive in the HC group. The CRI of NF-κB and its expression in liver tissues were positively correlated with the development of the liver fibrosis degree. The expression of NF-κB in the TH and TM groups significantly decreased. Therefore, we inferred that the mechanism of the antifibrotic effect of EPA might be mediated by reducing the expression of NF-κB in the liver tissue of rats with immune hepatic fibrosis, thus inhibiting the expression of the inflammatory factors IL-6 and ICAM-1 [52], alleviating the inflammatory reaction, and suppressing the expression of the collagen genes downstream of NF-κB [51].

In conclusion, the results of this experiment showed that EPA might reduce the serum levels of ALT and AST, decrease the serum concentrations of HA, LN, PC-III, and IV-C, and significantly improve morphological parameters of liver fibrosis. EPA might reduce liver inflammatory cell infiltration, decrease liver cell degeneration and necrosis, and reduce the formation of liver fibrous tissue hyperplasia. EPA might have a certain protective effect on rat liver fibrosis caused by pig serum. In our presented report, based on previous studies, we found that EPA might have a certain protective effect on rat liver fibrosis induced by pig serum, and CCl4. Our presented study found that TGF-β1, TIMP-1, NF-κB, and α-SMA were highly expressed in the liver fibrosis group rats and had relatively lower expression in the EPA treatment groups, the *P. notoginseng*/*S. mitiorrhiza* group and the colchicine group. The higher the degree of liver fibrosis corresponded with the higher the expression of TGF-β1, TIMP-1, NF-κB, and α-SMA. Therefore, EPA, a traditional Chinese drug, could prevent and treat hepatic fibrosis, and we inferred that its mechanism might be associated with the inhibition of the expression of TGF-β1, TIMP-1, NF-κB, and α-SMA. This could lead to the suppression of inflammatory factors during liver fibrosis, reducing inflammation, and blocking signal transduction pathways in the activation and proliferation of HSCs. Further in-depth studies of the relationship between EPA and hepatic fibrosis and its underlying mechanism are necessary for identifying new strategies for the prevention and treatment of hepatic fibrosis.

Author contributions

Dingchun Li: Conceptualization, Methodology, Validation, and Writing-Review & Editing; Dehongma Ma and Lihui Liu: experiment; Yihui Chen: Resources, Data Curation, and Data Entry; Ye Liu and Huaie Liu: Writing-Original Draft; Kexuan Chen and Jie Lu: Data Analysis and Data Curation; Lu Zhang: Visualization;Wu Li and Jing You: corresponding authors, supervision and research administration.

Folia Histochem Cytobiol. 2022
10.5603/FHC.a2022.0011
ISSN 0239-8508, e-ISSN 1897-5631

Financial support

This work was supported by grants from the Natural Foundation Surface Project of Yunnan Province (No. 2009CD087); the Yunnan Provincial Science and Technology Department-Kunming Medical University Joint Fund Key Project [No. 2017FE468 (-173)]; National Natural Science Foundation of China (82160801, 81760111,81760617) ; The Yunnan Province "Ten Thousands Program" Famous Doctor Special Project [Yunren Weifa (2020) No. 20, RLMY20200015].

Conflict of interest

No conflict of interest was declared by the authors.

References

1. Liu J, Liang W, Jing W, et al. Countdown to 2030: eliminating hepatitis B disease, China. Bull World Health Organ. 2019; 97(3): 230–238, doi: 10.2471/BLT.18.219469, indexed in Pubmed: 30992636.
2. Naik N, Madani A, Esteva A, et al. Deep learning-enabled breast cancer hormonal receptor status determination from base-level H&E stains. Nat Commun. 2020; 11(1): 5727, doi: 10.1038/s41467-020-19334-3, indexed in Pubmed: 33199723.
3. Shen T, Liu Y, Shang J, et al. Incidence and etiology of drug-induced liver injury in mainland China. Gastroenterology. 2019; 156(8): 2230–2241.e11, doi: 10.1053/j.gastro.2019.02.002, indexed in Pubmed: 30742832.
4. Fitzpatrick E. Non-alcoholic fatty liver disease. Oxford Medicine Online. 2018, doi: 10.1093/med/9780198759928.003.0061.
5. Roehlen N, Crouchet E, Baumert TF. Liver fibrosis: mechanistic concepts and therapeutic perspectives. Cells. 2020; 9(4), doi: 10.3390/cells9040875, indexed in Pubmed: 32260126.
6. Jiao J, Friedman SL, Aloman C. Hepatic fibrosis. Curr Opin Gastroenterol. 2009; 25(3): 223–229, doi: 10.1097/mog.0b013e3283279668, indexed in Pubmed: 19396960.
7. Friedman SL, Rockey DC, Bissell DM. Hepatic fibrosis 2006: report of the third AASLD single topic conference. Hepatology. 2007; 45(1): 242–249, doi: 10.1002/hep.21459, indexed in Pubmed: 17187439.
8. Huang M, Kim HG, Zhong X, et al. Sestrin 3 protects against diet-induced nonalcoholic steatohepatitis in mice through suppression of transforming growth factor β signal transduction. Hepatology. 2020; 71(1): 76–92, doi: 10.1002/hep.30820, indexed in Pubmed: 31215672.
9. Wan Y, Wu YL, Lian LH, et al. The anti-fibrotic effect of betulinic acid is mediated through the inhibition of NF-κB nuclear protein translocation. Chem Biol Interact. 2012; 195(3): 215–223, doi: 10.1016/j.cbi.2012.01.002, indexed in Pubmed: 22285267.
10. Li D, Li Wu, Chen Y, et al. Anti-fibrotic role and mechanism of Periplaneta americana extracts in CCl4-induced hepatic fibrosis in rats. Acta Biochim Biophys Sin (Shanghai). 2018; 50(5): 491–498, doi: 10.1093/abbs/gmy024, indexed in Pubmed: 29538616.
11. Li W, Duan L, He G, et al. [Prevention of CC14-induced liver fibrosis by Periplaneta americana extract]. Zhonghua Gan Zang Bing Za Zhi. 2009; 17(12): 948–950, doi: 10.3760/cma.j.issn.1007-3418.2009.12.017, indexed in Pubmed: 20038342.
12. Li W, Duan L, He G, et al. Effects of Periplaneta americana extract on experimental liver fibrosis. Lishizhen Medicine and Materia Medica Research. 2010; 21(5): 1137–1138, doi: 10.3969/j.issn.1008-0805.2010.05.052.
13. Iezzoni JC. Diagnostic histochemistry in hepatic pathology. Semin Diagn Pathol. 2018; 35(6): 381–389, doi: 10.1053/j.semdp.2018.10.003, indexed in Pubmed: 30409459.
14. Intraobserver and interobserver variations in liver biopsy interpretation in patients with chronic hepatitis C. The French METAVIR Cooperative Study Group. Hepatology. 1994; 20(1): 15–20, indexed in Pubmed: 8020885.
15. Liu L, Li W, Ma D, et al. Effect of American cockroach extract on NF-κB andα-SMA expression in CCl4 caused liver fibrosisrat model. Chongqing Medicine. 2014; 00(17): 015, doi: 10.3969/j.issn.1671-8348.2014.17.015.
16. Scheuer PJ. Classification of chronic viral hepatitis: a need for reassessment. J Hepatol. 1991; 13(3): 372–374, doi: 10.1016/0168-8278(91)90084-o, indexed in Pubmed: 1808228.
17. Ebrahimi H, Naderian M, Sohrabpour AA. New concepts on pathogenesis and diagnosis of liver fibrosis; a review article. Middle East J Dig Dis. 2016; 8(3): 166–178, doi: 10.15171/mejdd.2016.29, indexed in Pubmed: 27698966.
18. Zhou WC, Zhang QB, Qiao L. Pathogenesis of liver cirrhosis. World J Gastroenterol. 2014; 20(23): 7312–7324, doi: 10.3748/wjg.v20.i23.7312, indexed in Pubmed: 24966602.
19. Della Corte C, Aghemo A, Colombo M. Individualized hepatocellular carcinoma risk: the challenges for designing successful chemoprevention strategies. World J Gastroenterol. 2013; 19(9): 1359–1371, doi: 10.3748/wjg.v19.i9.1359, indexed in Pubmed: 23538741.
20. Ding J, Yu J, Wang C, et al. Ginkgo biloba extract alleviates liver fibrosis induced by CCl in rats. Liver Int. 2005; 25(6): 1224–1232, doi: 10.1111/j.1478-3231.2005.01169.x, indexed in Pubmed: 16343076.
21. Gao B, Bataller R. Alcoholic liver disease: pathogenesis and new therapeutic targets. Gastroenterology. 2011; 141(5): 1572–1585, doi: 10.1053/j.gastro.2011.09.002, indexed in Pubmed: 21920463.
22. Mederacke I, Hsu CC, Troeger JS, et al. Fate tracing reveals hepatic stellate cells as dominant contributors to liver fibrosis independent of its aetiology. Nat Commun. 2013; 4: 2823, doi: 10.1038/ncomms3823, indexed in Pubmed: 24264436.
23. Puche JE, Saiman Y, Friedman SL. Hepatic stellate cells and liver fibrosis. Compr Physiol. 2013; 3(4): 1473–1492, doi: 10.1002/cphy.c120035, indexed in Pubmed: 24265236.
24. Wells RG, Schwabe RF. Origin and function of myofibroblasts in the liver. Semin Liver Dis. 2015; 35(2): e1, doi: 10.1055/s-0035-1554915, indexed in Pubmed: 26008640.
25. Luk JM, Wang X, Liu P, et al. Traditional Chinese herbal medicines for treatment of liver fibrosis and cancer: from laboratory discovery to clinical evaluation. Liver Int. 2007; 27(7): 879–890, doi: 10.1111/j.1478-3231.2007.01527.x, indexed in Pubmed: 17696925.
26. Li CY, Chen YJ, Li SN, et al. Anti-hepatic fibrosis effects research on serum containing extracts of Periplaneta americana in vitr o]. Zhong Yao Cai. 2013; 36(5): 707–711.
27. Shi W, An Li, Zhang J, et al. extract ameliorates lipopolysaccharide-induced liver injury by improving mitochondrial dysfunction via the AMPK/PGC-1α signaling pathway. Exp Ther Med. 2021; 22(4): 1138, doi: 10.3892/etm.2021.10572, indexed in Pubmed: 34504584.
28. Zou Y, Zhang M, Zeng Di, et al. Extracts accelerate liver regeneration a complex network of pathways. Front Pharmacol. 2020; 11: 1174, doi: 10.3389/fphar.2020.01174, indexed in Pubmed: 32848780.
29. Wang K, Lin B, Brems JJ, et al. Hepatic apoptosis can modulate liver fibrosis through TIMP1 pathway. Apoptosis. 2013; 18(5): 566–577, doi: 10.1007/s10495-013-0827-5, indexed in Pubmed: 23456624.

30. Yang P, Niu Y. TGF-β1/Smad signaling pathway in tissue fibrosis:research advances. International Journal of Pharmaceutical Research. 2019; 46(10): 738–744, doi: 10.13220/j.cnki.jipr.2019.10.002.
31. Decologne N, Kolb M, Margetts PJ, et al. TGF-beta1 induces progressive pleural scarring and subpleural fibrosis. J Immunol. 2007; 179(9): 6043–6051, doi: 10.4049/jimmunol.179.9.6043, indexed in Pubmed: 17947678.
32. Seki E, De Minicis S, Osterreicher CH, et al. TLR4 enhances TGF-beta signaling and hepatic fibrosis. Nat Med. 2007; 13(11): 1324–1332, doi: 10.1038/nm1663, indexed in Pubmed: 17952090.
33. Liang Q, Lin Q, Li Y, et al. Effect of SIS3 on extracellular matrix remodeling and repair in a lipopolysaccharide-induced ARDS rat model. J Immunol Res. 2020; 2020: 6644687, doi: 10.1155/2020/6644687, indexed in Pubmed: 33294466.
34. Cheng K, Yang N, Mahato RI. TGF-beta1 gene silencing for treating liver fibrosis. Mol Pharm. 2009; 6(3): 772–779, doi: 10.1021/mp9000469, indexed in Pubmed: 19388665.
35. Baker AH, Edwards DR, Murphy G. Metalloproteinase inhibitors: biological actions and therapeutic opportunities. J Cell Sci. 2002; 115(Pt 19): 3719–3727, doi: 10.1242/jcs.00063, indexed in Pubmed: 12235282.
36. Stetler-Stevenson WG. The tumor microenvironment: regulation by MMP-independent effects of tissue inhibitor of metalloproteinases-2. Cancer Metastasis Rev. 2008; 27(1): 57–66, doi: 10.1007/s10555-007-9105-8, indexed in Pubmed: 18058195.
37. Friedman SL. Hepatic stellate cells: protean, multifunctional, and enigmatic cells of the liver. Physiol Rev. 2008; 88(1): 125–172, doi: 10.1152/physrev.00013.2007, indexed in Pubmed: 18195085.
38. Fowell AJ, Collins JE, Duncombe DR, et al. Silencing tissue inhibitors of metalloproteinases (TIMPs) with short interfering RNA reveals a role for TIMP-1 in hepatic stellate cell proliferation. Biochem Biophys Res Commun. 2011; 407(2): 277–282, doi: 10.1016/j.bbrc.2011.02.009, indexed in Pubmed: 21300026.
39. Rippe RA, Brenner DA. From quiescence to activation: gene regulation in hepatic stellate cells. Gastroenterology. 2004; 127(4): 1260–1262, doi: 10.1053/j.gastro.2004.08.028, indexed in Pubmed: 15481004.
40. Zhang Y, Xu N, Xu J, et al. E2F1 is a novel fibrogenic gene that regulates cholestatic liver fibrosis through the Egr-1/SHP/EID1 network. Hepatology. 2014; 60(3): 919–930, doi: 10.1002/hep.27121, indexed in Pubmed: 24619556.
41. Foo NP, Lin SH, Lee YH, et al. α-Lipoic acid inhibits liver fibrosis through the attenuation of ROS-triggered signaling in hepatic stellate cells activated by PDGF and TGF-β. Toxicology. 2011; 282(1-2): 39–46, doi: 10.1016/j.tox.2011.01.009, indexed in Pubmed: 21251946.
42. Kong D, Zhang F, Zhang Z, et al. Clearance of activated stellate cells for hepatic fibrosis regression: molecular basis and translational potential. Biomed Pharmacother. 2013; 67(3): 246–250, doi: 10.1016/j.biopha.2012.10.002, indexed in Pubmed: 23201010.
43. Park JS, Oh Y, Park YJ, et al. Targeting of dermal myofibroblasts through death receptor 5 arrests fibrosis in mouse models of scleroderma. Nat Commun. 2019; 10(1): 1128, doi: 10.1038/s41467-019-09101-4, indexed in Pubmed: 30850660.
44. Dunphy G, Flannery SM, Almine JF, et al. Non-canonical activation of the DNA sensing adaptor STING by ATM and IFI16 mediates NF-κB signaling after nuclear DNA damage. Mol Cell. 2018; 71(5): 745–760.e5, doi: 10.1016/j.molcel.2018.07.034, indexed in Pubmed: 30193098.
45. Iida Y, Ciechanover A, Marzese DM, et al. Epigenetic Regulation of KPC1 Ubiquitin Ligase Affects the NF-κB Pathway in Melanoma. Clin Cancer Res. 2017; 23(16): 4831–4842, doi: 10.1158/1078-0432.CCR-17-0146, indexed in Pubmed: 28389511.
46. Song W, Xu J, Xu R, et al. Expression and distribution of NF-κB in experimental hepatic fibrosis. Chinese Journal of Pathophysiology. 2010; 26(1): 12–16.
47. Khattar E, Maung KZ, Chew CLi, et al. Rap1 regulates hematopoietic stem cell survival and affects oncogenesis and response to chemotherapy. Nat Commun. 2019; 10(1): 5349, doi: 10.1038/s41467-019-13082-9, indexed in Pubmed: 31836706.
48. Li L, Wei J, Mallampalli RK, et al. TRIM21 mitigates human lung microvascular endothelial cells' inflammatory responses to LPS. Am J Respir Cell Mol Biol. 2019; 61(6): 776–785, doi: 10.1165/rcmb.2018-0366OC, indexed in Pubmed: 31184939.
49. Scirpo R, Fiorotto R, Villani A, et al. Stimulation of nuclear receptor peroxisome proliferator-activated receptor-γ limits NF-κB-dependent inflammation in mouse cystic fibrosis biliary epithelium. Hepatology. 2015; 62(5): 1551–1562, doi: 10.1002/hep.28000, indexed in Pubmed: 26199136.
50. Yu Y, Luo Y, Fang Z, et al. Mechanism of sanguinarine in inhibiting macrophages to promote metastasis and proliferation of lung cancer via modulating the exosomes in A549 cells. Onco Targets Ther. 2020; 13: 8989–9003, doi: 10.2147/OTT.S261054, indexed in Pubmed: 32982290.
51. Elsharkawy AM, Mann DA. Nuclear factor-kappaB and the hepatic inflammation-fibrosis-cancer axis. Hepatology. 2007; 46(2): 590–597, doi: 10.1002/hep.21802, indexed in Pubmed: 17661407.
52. Pillon NJ, Azizi PM, Li YE, et al. Palmitate-induced inflammatory pathways in human adipose microvascular endothelial cells promote monocyte adhesion and impair insulin transcytosis. Am J Physiol Endocrinol Metab. 2015; 309(1): E35–E44, doi: 10.1152/ajpendo.00611.2014, indexed in Pubmed: 25944880.

Submitted: 19 January, 2022
Accepted after reviews: 6 May, 2022
Available as AoP: 16 May, 2022